The Journal of Supercomputing
https://doi.org/10.1007/s11227-019-02922-6

Land use classification from social media data and satellite imagery

Yaqin Ye[1] · Ying An[1] · Bo Chen[2] · JunJue Wang[1] · Yingqiang Zhong[1]

Abstract
Detailed urban land use classification plays a highly important role in the development and management of cities and in the identification of human activities. The complexity of the urban system makes its functional zoning a challenge, which makes such maps underutilized. A detailed land use classification encompasses both the natural land features and the classification of structures closely related to human activities. The use of satellite imagery to classify land use can effectively benefit the recognition of natural objects, but its performance demands significant improvement in the recognition of social functions due to the lack of information regarding human activities. To identify such activities in an urban area, we added Point of Interests (POI) data. This dataset contains both geographical tags and attributes that describe human activities. However, it has an uneven spatial distribution, with gaps in coverage being readily apparent. This paper proposes a land use classification framework using satellite imagery and data from social media. The proposed method employs a kernel density estimation to handle the spatial unevenness of POI data. The solution of mixed programming of MPI and OpenMP was adopted to parallel the algorithm. The results are compared to data compiled manually by means of human interpretation. Considering the example of Wuhan city, results show that the overall accuracy of land use type classification is 86.2%, and the Kappa coefficient is 0.860. It is demonstrated that using both POI and satellite images, a detailed land use map can be created automatically with satisfactory robustness.

Keywords Land use · Point of Interests · Satellite image · Classification

✉ Yaqin Ye
yeyaqin@126.com; yeyaqin@cug.edu.cn

[1] China University of Geosciences, Wuhan 430074, China

[2] Wuhan ZondyCyber Technology Co., Ltd., Wuhan 430074, China

Published online: 06 June 2019

1 Introduction

In the past decades, urbanization accelerated significantly and the number of large cities continues to increase [1]. Urbanization introduces significant challenges to the environment, the healthcare system, and the transportation. Land use maps are traditionally derived from high spatial resolution remote sensing imagery and aerial photography or from data collected in field trips. Producing such maps is time-consuming and expensive. An updated land use map with most recent information is needed for managing and planning city development. This paper aims at addressing the automatic land use mapping problem by leveraging satellite imagery and social media data.

Studies of land use focus on the social aspects of the landscape. Despite that the remote sensing data have been used in the classification of land cover [2–4], classification of land use is beyond the distinction among features such as lakes, farmland, and building. It includes additional features, e.g., commercial areas, residential areas, and industrial parks. That is, land use is closely related to human activities; therefore, data capturing human activities are the key to land use analysis. Yet, such social attributes are usually absent from most of the remote sensing data.

With the development of networking technologies and ubiquitous sensing, a large volume of user-generated data became available, which are known as spontaneous geographic information using a smart device with GPS functions and are based on the openly accessible reference data. Open Street Maps, Wikipedia maps, and Google Map Maker are examples of web-based projects that collect and manage spontaneous geographic information and allow users to create new or update the existing geographic data. These data scaffold new opportunities for automatic construction of land use maps.

Point of Interest (POI) has been used to annotate significant landmarks on a map such as government agencies, companies, shopping malls, and restaurants. As POIs describe geographic entities with attributes such as coordinates, addresses, and names, they greatly enhance the presentation of maps for urban social activities [5]. Yuan et al. [6] proposed a grid-based method to identify areas by function based on taxi track data and POIs. Han et al. [7] identified functional areas using data on population movements and POIs in Beijing. Both studies focus on the identification of a single land use type. Chi et al. [8] proposed a method for recognizing mixed-use areas based on POIs and identifying functional areas in Wuhan. The method divides the study area into equal squares of 1000 m by 1000 m without considering the adjacency of urban function zones. It relies extensively on the potentially inaccurate discretization of the available data. Some methods are proposed for mining POI semantic features [9–11]. However, the sparsity and uneven distribution of the POIs pose a great challenge for land use analysis. Integrating satellite imagery and social media data brings new opportunities to land use classification by leveraging the physical properties of the land surface derived from images with dense coverage and the socioeconomic attributes of social media.

2 Study area and datasets

The study area used in our experiments is Wuhan city, which is the capital of Hubei, China. Both satellite images and POIs are obtained. The satellite image of Wuhan with a spacial resolution of 10 m (depicted as the background image of Fig. 1) is downloaded from Google Maps. More than 300,000 POIs in 2012 are retrieved, where each point contains the functional and location attributes. The spatial distribution of all POIs is shown in Fig. 1a. The POIs are put into six categories including residential area, public service, commercial service, industrial area, transportation service, and park. Figure 2 illustrates the zoom-in view of the POIs of commercial and transportation services. It is clear that the POIs are highly uneven within a type and between types.

In addition to the satellite images and POI data, road networks from the OpenStreetMap (OSM) are obtained as auxiliary data for identifying urban functional units. The data from OpenStreetMap includes spatial and attribute components. The spatial component includes three data types: Nodes, Ways, and Relations. The road network is in the vector format and contains highway, main road, primary road, secondary road, tertiary road, and primary-link road.

3 Proposed method

The land use of a region in a city is decided by its urban functions [12]. According to the existence of the POI data, we divide an urban space into single-use areas, mixed-use areas, and areas without POI data. A single-use area is one that encloses

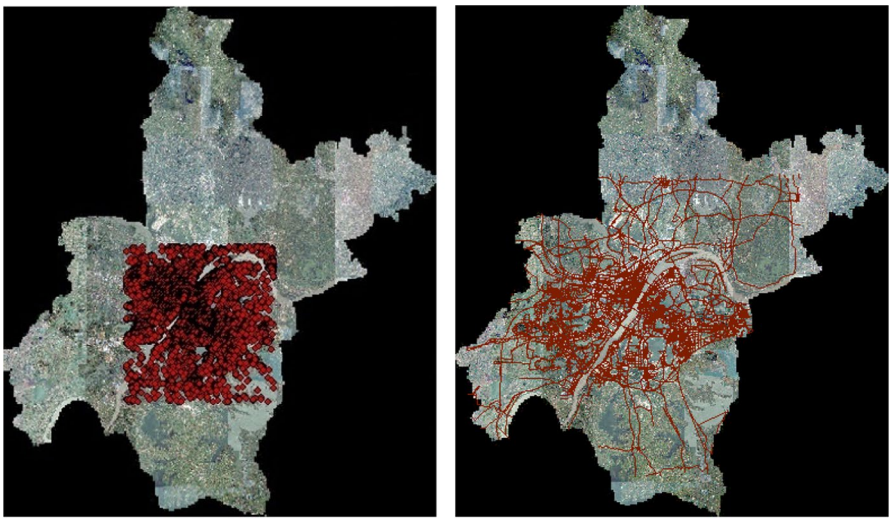

(a) POI points distribution **(b)** OSM data

Fig. 1 POI and OSM data of the study area superimposed on a satellite image of Hubei, China

Fig. 2 The uneven distributions of commercial and transportation services. Left: commercial service POIs. Right: transportation service POIs

a dominated type of POIs. A mixed-use area is one that contains two or more types of POIs of competitive numbers. The area without POI data is classified using extensional information from their neighbors.

Figure 3 illustrates the architecture of the proposed method, called Hierarchical Determination method based on Kernel Density Classification (KDC-HDM). In KDC-HDM method, the road network from OSM is used to generate the basic block for land use classification, namely functional unit (FU). For each FU, if there exist POI data, a decision is made according to the types of the POIs; otherwise, classification of the satellite image is used to decide build-up and non-built-up areas and kernel density-based classification of the POIs is used to decide the land use type of built-up area.

3.1 Urban functional units

A parcel is the basic unit of urban management in a city's administrative system. The boundaries of cartographic units are usually determined by field trips, which is a process that requires considerable effort and is time-consuming. Parcels outline the boundary of the land where buildings are located in. It divides the land into very small regions that many parcels have no POI annotations, which makes POI-based land use classification infeasible. In our method, we use the road networks from OSM to generate urban functional units, similar to traffic analysis zones. The scope of an FU is usually greater than that of a parcel.

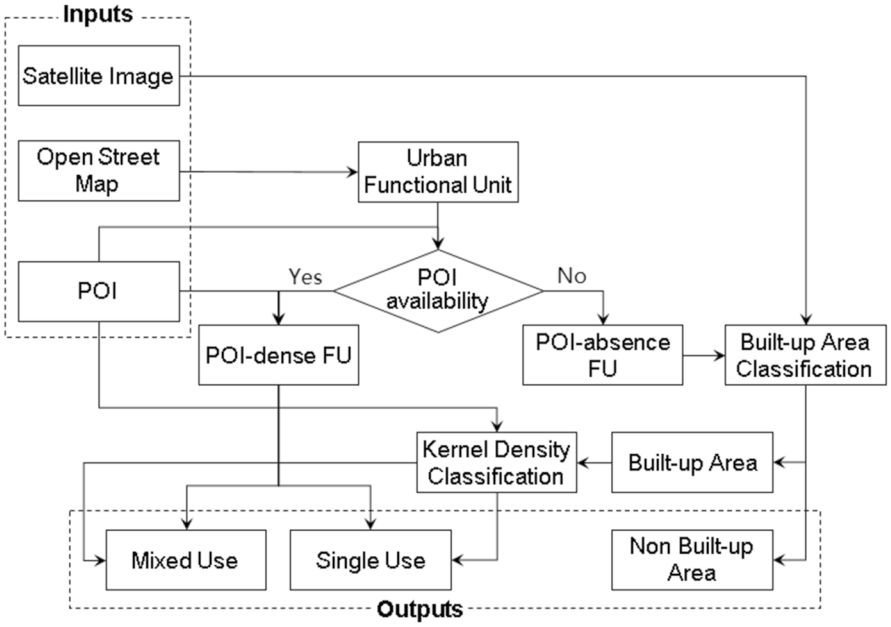

Fig. 3 The flowchart of the proposed method

In OSM data, there exist dangling lines. To avoid erroneous FUs generated from irrelevant data, ArcGIS Topology tools are used to identify and remove dangling lines. In addition, a point on a suspension line is deleted if the suspension line segment starting at this point spans less than 500 m. If lines appear to belong to one of two parallel lines that are 100 m long and are disconnected from any other lines, they are removed as well. OSM data also include two-way roads that are very close to each other, which produce long, narrow street blocks that are false and shall be removed. Road buffer is applied to different types of streets and the street categorization is listed in Table 1. According to the road width, the redundant lines within the buffer are removed.

Table 1 Road categorization

Category	Description	Width
Motorway	A restricted access major divided highway.	55
Primary	The 2nd most important roads in a country's system	30
Secondary	The 3rd most important roads in a country's system	20
Tertiary	The next 4th important roads in a country's system	10
Ramps	The roads leading from a road to another road.	20
Unclassified	The least important roads in a country's system.	10

The width is in meters

Urban FUs are created from the cleaned OSM road network using the topology building tools. After the road network passed the topology checker, the topology building tool is used to generate FUs. An example of FUs is shown in Fig. 4.

3.2 Land use classification of POI-dense FUs

The POI data consists of many categories, which are heavily overlapped. For example, dormitory exists as part of a residential area as well a part of a school, which is considered as educational services. As the consequence, the raw data needs to be recategorized. In this study, we recategorized the POI points into 13 groups: catering, scenic location, public facility, business, shopping, transportation facility, education, commercial housing facility, lifestyle, sport, medical, government, and accommodation. Additionally, POIs with a low popularity, such as bus stations, public restrooms, and logistics, are excluded. Following the POI classification in [13], the POI data are divided into six categories as listed in Table 2. We associate the existing POI types to the level II and level III types in Table 2, then classify all POIs as the corresponding level I categories and finally get six POI categories.

Each FU may contain multiple types of POIs and they are weighted differently. To avoid bias from the count of POI points, we use a kernel density function. The normalized POIs density is computed as follows:

$$p_i = \frac{n_i/N_i}{\sum_j n_j/N_j}, \tag{1}$$

where i denotes the POI category of an FU and n_i denotes the number of POIs of type i within the FU, N is the number of all POIs. The land use represented by the type-i POIs is the primary land use type of the FU if $p_i \geq \epsilon$, and such FU is decided to be a single-use area. If the largest p_i is less than ϵ and there exist more than one p_i, the FU is classified as a mixed-use area. Densities of all types of POIs in each FU are sorted. The highest two types are used to represent the land use type of the

Fig. 4 Functional units generated from OSM. Each enclosed cell is a functional unit

Table 2 POI categories of built-up areas

Level I	Level II	Level III
Residential	Residential area and business related	Dormitories, villas, residential, quarters, community centers
Industrial	Company and business residence	Factory, company, industrial park
Commercial	Catering, shopping, accommodation, finance, etc.	Restaurant related; shopping mall; hotels, bank, insurance company
Public service	Education, sports service, health care, etc.	School, library, museum; cinema, hospital, government agencies, social organizations, vehicles management
Transportation	Transportation service facilities and road facilities	Station, airport, dock, tool booths, services area
Park	Park plaza and tourist sites	Parks, squares, botanical gardens, zoos, attractions

mixed-use area. If all p_i values in the FU are zeros, such FU is decided as an unclassified area. In our experiments, we set ϵ as 0.6. according to Chen [14].

3.3 Land use classification of POI-absence FUs

To overcome the absence of POI in an FU, we classify the land into built-up and non-built-up areas from the satellite images using color, shape, and size features. Lands that include man-made structures are classified into built-up and non-built-up areas, and we leverage POI density in the surrounding areas to decide the land use type of a POI-absence FU of built-up areas. The kernel density function embeds the distance-based attenuation following the first law of geography, which states that all attributes on a geographic surface are inter-related and closer values imply a stronger relation than the distant ones [15]. The attenuation is a function of distance and depends on the location of the distribution. The kernel density function $f(s)$ at position s is computed as follows:

$$f(s) = \frac{1}{h^2} \sum_{i=1}^{n} \phi\left(\frac{s - c_i}{h}\right), \tag{2}$$

where h is the attenuation threshold, n is the number of POIs within the distance of h, and $\phi(\cdot)$ is the spatial weight function in the following form:

$$\phi(x) = 0.75(1 - x^2). \tag{3}$$

The attenuation threshold h is computed as follows:

$$h = \frac{\alpha}{n^2} \min\left(\sigma, \frac{D_m}{\sqrt{\ln 2}}\right), \tag{4}$$

$$\sigma = \sqrt{\frac{1}{n} \sum_{i=1}^{n} [(x_i - \bar{X})^2 + (y_i - \bar{Y})^2]}, \tag{5}$$

where $\alpha = 0.9$, x_i and y_i are the coordinates of the element i, $\bar{X}, \bar{Y}$ are the average of the input points, n is the total number of elements and D_m is the median distance from the center to all points.

The land use type of a POI absence, built-up FU is decided by the land use type of its adjacent FU that has the greatest kernel density. To calculate the kernel density, for each POI class, a grid is created and processed as follows:

- A search radius h [a.k.a, attenuation threshold, and determined by formulas (4) and (5)] is defined.
- The distances from the center of each cell to the center of the adjacent cells are calculated. All adjacent cells within the radius are considered.

- The density of each occurrence element and the centers of adjacent cells are calculated following the kernel function, attenuation distance and the number of occurrence entities.
- At the center of each cell, the density of the same type is allocated to the cell. For other land use types, the default density is zero.

Figure 5 illustrates an example of applying kernel density for land use classification. The target FU is the input and highlighted in green. Adjacent FUs are depicted with thick borders and the center is marked with a dot. The density of the six land use types of the adjacent FUs is computed. The blue and light green colors represent different densities of the land use types. The adjacent FU with the highest density (depicted in red color on the output) is used to make land use classification of the target FU.

3.4 The parallelization processing of KDC-HDM algorithms

By analyzing the type determination process of each urban block in KDC-HDM, the blocks are independent in space and can be processed in parallel optimization, especially in the type determination process of a single built-up area. Because the space is independent, the calculation process is similar, and the data coupling degree is low, parallel processing can be used to improve the efficiency of the algorithm. First, we need to divide the whole city into several subplots. According to the number of CPU cores and GPU cores in the cluster, the number of blocks allocated by each node is determined. Although the core number of independent graphics cards supporting CUDA is much larger than that of CPU, independent graphics cards are not necessarily configurable on all node computers in the cluster. In order to maximize the parallel computing power of cluster, it is necessary to allocate different number of blocks according to whether there are independent graphics cards in the nodes and provide different parallel schemes. Assuming that J nodes in the cluster are equipped with independent graphics cards, K nodes have no independent graphics cards, and there are M urban blocks in total. Each node is allocated

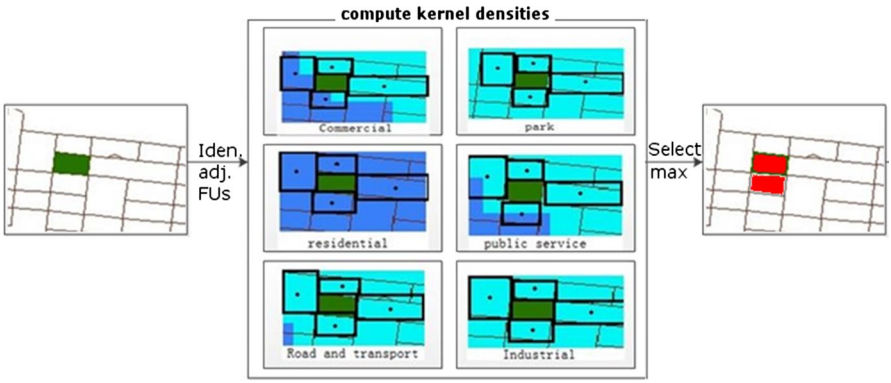

Fig. 5 Land use classification using the kernel density of the adjacent FUs (color figure online)

an independent subplot and the number of subplots are $J + K$. At this time, the key problem is to determine the blocks in each sub-block group, that is, the number of blocks in sub-block group. The core number of SPCUDA Core with GPU node is G_j, the total number of threads of independent graphics card is $\sum_{j\in J} G_j$, the core number of CPU without independent graphics card is C_k, and the core number of CPU is $\sum_{k\in K} C_k$. So, the number of blocks to be processed by each core is $M/(\sum_{j\in J} G_j + \sum_{k\in K} C_k)$. The number of blocks in the subplot with independent graphics card node is $M/(\sum_{j\in J} G_j + \sum_{k\in K} C_k)^* G_j$, while the number of blocks in the subplot without independent graphics card node is $M/(\sum_{j\in J} G_j + \sum_{k\in K} C_k)^* C_k$. For nodes without CUDA independent graphics cards, their parallel ability mainly comes from the multi-core CPU. This paper adopts the mixed program solution of MPI (Message Passing Interface) and OpenMP (Open Multiprocessing), and uses the # pragma OMP parallel clause to realize the task scheduling of subplot in nodes. For nodes equipped with CUDA independent graphics cards, we can use CUDA to give full play to the computing power of GPU multi-core.

4 Experimental results

Figure 6 depicts the resulted land use map of Wuhan using our proposed method. The primary land use types are numbered one through six, and the numbers above ten denote mixed-use types. For instance, "12" denotes the mixed-used of the primary types one and two. The types seven through ten are non-built-up areas including farm land, undeveloped land, lake, and green land, respectively.

4.1 Accuracy of single-use area

In our dataset, the proportion of single-use land is 71%, the proportion of mixed-use land is 11%, and the proportion of land without POI is 18%. The FUs of single-use type account for 56%, the mixed-use type is 23%, and non-built-up areas are 21%. The overall accuracy of our method is 86.2%, and the Kappa coefficient is 0.86. We compare our results with the Amap for accuracy analysis. Table 3 presents the confusion matrix of land use classification including the non-built-up areas. In this table, UA stands for user's accuracy, which measures the percentage of the number of pixels in the category when the classified land cover category corresponds to real ground reference data. PA stands for producer's accuracy, which measures the instances belonging to a land-covered category that are misclassified. The UA represents a prediction accuracy of the classification without knowing the true value. The PA represents the classification accuracy when the true value becomes known. The minimum user's accuracy is 73% for land use type public service and the maximum user's accuracy is 96% for land use type farm. As to the producer's accuracy, both land use types public service and green land reached 100% and the minimum user's accuracy is 71% for land use type residential. The overall accuracy reaches 86.2%.

The land use classification chart includes six categories and the confusion matrix in Table 3 lists the accuracy of land use classification of the built-up areas. As shown

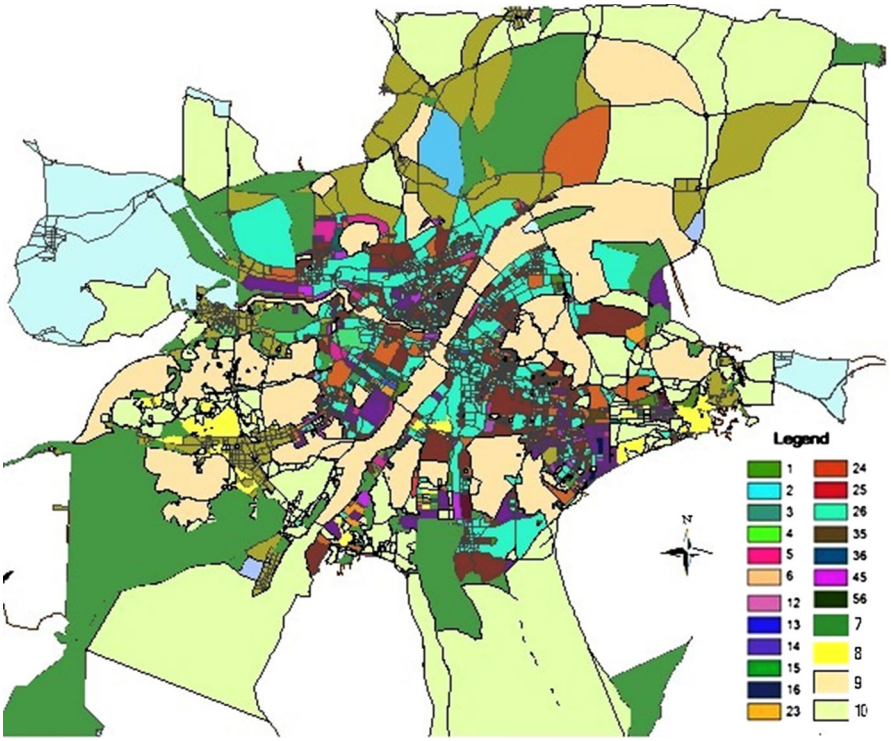

Fig. 6 Land use classification. Color denotes different land use types (color figure online)

Table 3 The confusion matrix of land use classification of Wuhan

LU	Tran.	Ind.	Res.	Pub.	Park	Com.	Farm	Und.	Lake	Gre.	UA (%)
Tran.	30	2	2	–	2	–	–	–	–	–	83
Ind.	–	30	4	–	–	1	–	–	–	–	86
Res.	–	3	25	–	–	3	–	–	–	–	81
Pub.	1	–	2	8	–	–	–	–	–	–	73
Park	1	–	–	–	15	2	–	–	–	–	83
Com.	–	–	1	–	1	22	–	–	–	–	92
Farm	–	–	–	–	–	–	24	1	–	–	96
Und.	1	–	–	–	–	1	1	20	–	–	87
Lake	1	–	–	–	–	1	–	1	20	–	87
Gre.	1	–	1	–	–	–	–	–	1	24	89
PA (%)	86	86	71	100	83	73	96	91	95	100	86.2

For clarity, the dashes '–' in this table are zeros

in Table 3, under the premise of comparison with other types of PA, the recognition accuracy of residential land and commercial land is relatively low.

4.2 Accuracy of mixed-use area

As shown in Fig. 7, we arbitrarily selected 82 samples from Google Street view, among which 57 samples are mixed-use types and 25 samples are single-use types. Among the selected samples, 17 mixed-use FUs were misclassified as single-use types. The recognition accuracy of the 40 samples is calculated by comparing the classification results with what is observed on the panoramic map obtained from the Google Map and high-resolution remote sensing imagery. The recognition of single-use areas is 70% and the recognition of mixed-use areas is 58%.

4.3 Analysis of POI-absence area

The conventional method faces the difficulty of estimating the land use type of areas without POIs. According to the first law of geography, the kernel density analysis of the surrounding buildings is more affected by objects in a closer distance. By comparing the traditional urban functional area identification model, it can be seen that the research model solved the no-POI area and the data shows that the proportion of unidentified areas is reduced from 33.34 to 0.26%.

Fig. 7 The test samples

Table 4 The confusion matrix of classification of Hongshan District by AlexNet

LU	Tran.	Ind.	Res.	Pub.	Park	Com.	Farm	Und.	Lake	Gre.	UA (%)
Tran.	68	8	7	2	1	–	7	–	6	1	68
Ind.	11	103	75	85	15	5	7	1	105	93	21
Res.	19	101	306	261	21	2	3	4	190	93	31
Pub.	1	100	166	370	9	3	5	8	35	3	31
Park	53	1	5	9	128	–	–	1	1	2	64
Com.	1	51	2	3	2	38	–	–	3	–	38
Farm	4	8	72	30	28	–	56	2	–	–	28
Und.	1	1	1	1	–	1	1	93	1	–	93
Lake	10	108	121	37	9	4	78	1	428	4	54
Gre.	1	84	–	4	8	1	–	13	89	200	45
PA (%)	40	18	41	46	58	70	36	76	56	31	46

For clarity, the dashes '–' in this table are zeros

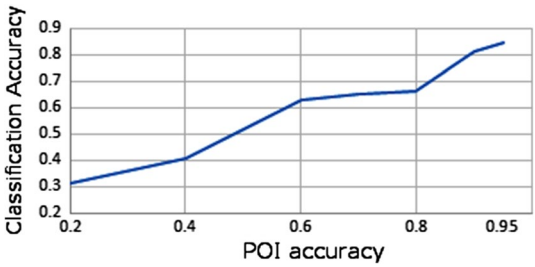

Fig. 8 The classification accuracy with respect to the accuracy of POIs

We employed AlexNet to classify the satellite image data with a pixel size of 10 m × 10 m. We adopt the training set from places365 and divide data set into a grid of 50 m × 50 m. Compared with the previous spatial subdivision method by the road network, this division method cuts the area into smaller cells. From the confusion matrix shown in Table 4, the recognition accuracy of the undeveloped area is 93% and the overall accuracy is 46%. The experimental results show that the effect on the built-up area with insignificant features is not so good. This demonstrates the necessity of integrating POI for land functional area identification. The method proposed in this paper improves the classification accuracy from 46 to 86.2%.

4.4 POI quality

We conducted experiments to study the impact of POI data accuracy on the land use classification performance. We extracted the POI data with the accuracy of 20%, 40%, 60%, 80%, and 95%, and evaluate the accuracy of land use classification. The results are shown in Fig. 8. It is clear that the accuracy of the land use classification is mostly linearly proportional to the accuracy of the POI in general. When the POI

accuracy is greater than 80%, the classification accuracy changes little as the POI accuracy increases, and the classification accuracy is reached about 85%.

We select a set of data in the Hongshan District, Wuhan and reduced the accuracy of POIs to 60% manually by introducing incorrect POI labels. The above experimental procedure is repeated to obtain the final result and the confusion matrix, as shown in Fig. 9 and Table 5. The Kappa coefficient of Table 5 is 0.592. Compared with Table 3, the accuracy drops.

5 Conclusions

This study combines the characteristics of image data and the social characteristics of POIs and proposes a multi-feature fusion land use classification model to improve land use classification. The physical (e.g., color and texture)

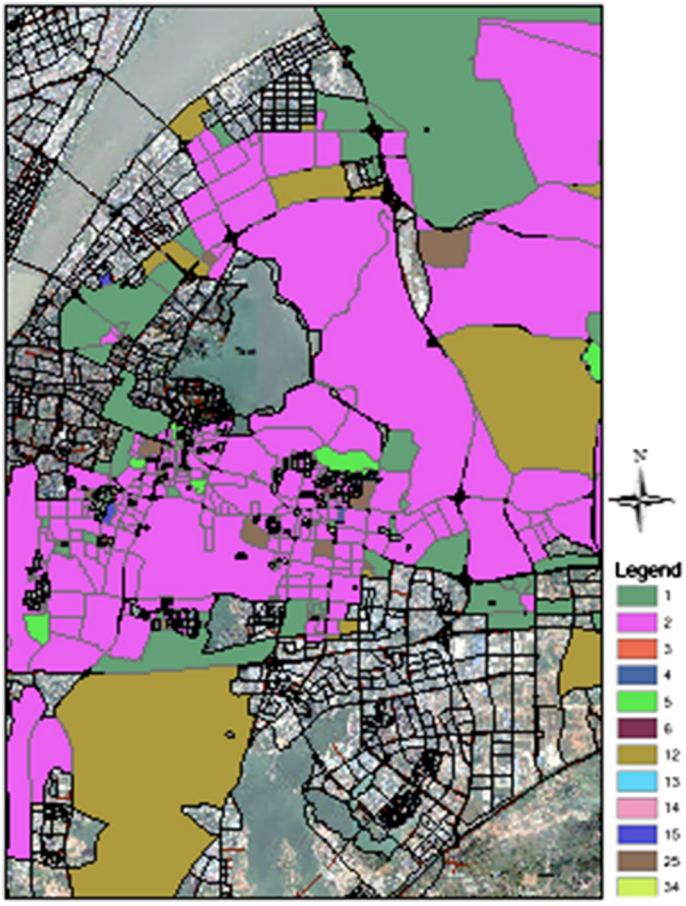

Fig. 9 The classification of Hongshan District

Table 5 The confusion matrix of classification of the primary land use types in the Hongshan District

Land use	1	2	3	4	5	6	UA(%)
1	6	–	–	1	1	2	60
2	–	16	1	1	–	2	80
3	–	1	15	–	4	–	75
4	1	1	4	12	1	1	60
5	2	–	5	2	10	1	50
6	1	1	1	1	1	5	50
PA (%)	60	84	58	71	59	45	64

For clarity, the dashes '–' in this table are zeros

characteristics and social (e.g., socioeconomic) attributes required for land use maps can be extracted from satellite imagery and social media data, respectively. The use of kernel density function to characterize the influence of POI on the surrounding area is proposed, and the spatial reasoning of the land type in the blank area and the mixed-use area is performed by means of neighborhood information, which identifies mixed-use areas and classify single-use area accurately. The solution of mixed programming of MPI and OpenMP is adopted to parallel the algorithm. Combining all methods results in improved accuracy of land use classification. Our proposed method achieves a more accurate classification of land use. The overall accuracy of our method is 86.2%, and the Kappa coefficient is 0.86. The minimum user's accuracy is 73% for public service, and the maximum user's accuracy is 96% for farms. The producer's accuracy for both public service and green land achieves 100%, and the minimum user's accuracy is at 71% for residential areas. The overall accuracy achieves 86.2%. The recognition of single-use areas is 70%, and the recognition of mixed-use areas is 58%. By comparing the result of the traditional urban functional area identification model, our present study with the kernel density urban functional area model reduced the proportion of unidentified areas from 33.34 to 0.26%. Compared with AlexNet, our method performs well in the classification of built-up areas and improves the accuracy of classification from 64 to 86.2%. The accuracy of POI influences the classification results. From the experimental results, the accuracy of POI should be at least 60% or above.

Funding This research was funded by the National Natural Science Foundation of China, Grant Nos. 41301426, 41301427, 41371422 and National Key Research and Development Program of China, Project Nos. 2016YFB0502304, 2017YFB050380504.

Compliance with ethical standards

Conflict of interest The authors declare no conflict of interest.

References

1. Hu T, Yang J, Li X, Gong P (2016) Mapping urban land use by using landsat images and open social data. Remote Sens 2:151
2. Yuan X, Sarma V (2011) Automatic urban water body detection and segmentation from sparse ALSM data via spatially constrained, model-driven clustering. IEEE Geosci Remote Sens Lett 8:75–77
3. Gong Y, Liu Y, Lin Y, Yang J (2012) Exploring spatiotemporal characteristics of intra-urban trips using metro smartcard records. In: IEEE International Conference on Geoinformatics, pp 1–7
4. Fang F, Yuan X, Wang L, Liu Y, Luo Z (2018) Urban land-use classification from photographs. IEEE Geosci Remote Sens Lett 15:1927–1931
5. Gu Z, Chen X, Yang H (2011) Study on spatial clustering algorithm for division of urban functional areas. Sci Geom 36:65–67
6. Yuan J, Zheng Y, Xie X (2012) Discovering regions of different functions in a city using human mobility and POIs. In: ACM SIGKDD International Conference on Knowledge Discovery and Data Mining, pp 186–194
7. Yuying H, Xiang Y, Wei L (2016) Functional area identification based on Beijing Bus Credit Card Data and Points of Interest. City Plan 40:52–60
8. Chi CA, Clark DA, Lee S, Biron D, Luo L, Gabel CV, Brown J, Sengupta P, Samuel A (2007) Temperature and food mediate long-term thermotactic behavioral plasticity by association-independent mechanisms in *C. elegans*. J Exp Biol 210:4043–4052
9. Liu X, He J, Yao Y, Zhang J, Liang H, Wang H, Hong Y (2017) Classifying urban land use by integrating remote sensing and social media data. Int J Geogr Inf Sci 31:1675–1696
10. Zhang X, Du S, Wang Q (2017) Hierarchical semantic cognition for urban functional zones with VHR satellite images and POI data. ISPRS J Photogramm Remote Sens 132:170–184
11. Yao Y, Li X, Liu X, Liu P, Liang Z, Zhang J, Mai K (2017) Sensing spatial distribution of urban land use by integrating points-of-interest and Google Word2Vec model. Int J Geogr Inf Sci 31:825–848
12. Tao P, Sobolevsky S, Ratti C, Shaw S, Li T, Zhou C (2014) A new insight into land use classification based on aggregated mobile phone data. Int J Geogr Inf Sci 28:1988–2007
13. Gong P, Howarth P (1990) The use of structural information for improving land-cover classification accuracies at the rural–urban fringe. Photogramm Eng Remote Sens 56:67–73
14. Chen B, Huang B, Xu B (2017) Multi-source remotely sensed data fusion for improving land cover classification. ISPRS J Photogramm Remote Sens 124:27–39
15. Shaban MA, Dikshit O (2001) Improvement of classification in urban areas by the use of textural features: the case study of Lucknow city, Uttar Pradesh. Int J Remote Sens 22:565–593